Polymer Chemistry

A Highly Efficient Metal-Free Protocol for the Synthesis of Linear Polydicyclopentadiene

Journal:	*Polymer Chemistry*
Manuscript ID	PY-ART-02-2021-000191.R1
Article Type:	Paper
Date Submitted by the Author:	23-Mar-2021
Complete List of Authors:	Yang, Xuejin; University of Wisconsin-Madison, Chemistry Murphy, Laura; University of Washington Tacoma, Division of Sciences and Mathematics, School of Integrated Arts and Sciences Haque, Farihah; Tulane University, Chemistry; University of Minnesota Twin Cities, Chemistry Grayson, Scott; Tulane University, Chemistry Boydston, Andrew; University Of Wisconsin Colleges, Chemistry; University of Wisconsin-Madison, Department of Chemical and Biological Engineering, Department of Materials Science and Engineering

ARTICLE

A Highly Efficient Metal-Free Protocol for the Synthesis of Linear Polydicyclopentadiene

Received 00th January 20xx,
Accepted 00th January 20xx

DOI: 10.1039/x0xx00000x

Xuejin Yang,[a] Laura M. Murphy,[b] Farihah M. Haque,[c,d] Scott M. Grayson,[c] Andrew J. Boydston*[a,e]

We have achieved breakthroughs for the efficient synthesis of linear polydicyclopentadiene (pDCPD) via photoredox mediated metal-free ring-opening metathesis polymerization (MF-ROMP). Molecular weight control from 1 to 16 kDa can be targeted in a straightforward manner. Assisted by this method, the T_g–M_n dependence of linear pDCPD is investigated and reported for the first time.

Introduction

Polydicyclopentadiene (pDCPD) is typically produced as a thermoset using metal-based olefin metathesis catalysts and commercially available *endo*-DCPD (*endo*-**1**). Classic transition metal initiators usually produce insoluble, cross-linked pDCPD networks (Scheme 1). Cross-linking is achieved by secondary metathesis or thermally induced olefin-addition reactions involving the low strain cyclopentene moiety, although the detailed mechanism is yet to be fully understood.[1–5] As a thermoset material, the cross-linking of pDCPD accounts for its high glass transition temperature (T_g = 114−165 °C).[5–7] Reported T_g values vary widely depending on preparation conditions and cross-linking density.[8,9] Notably high T_gs (210 °C) were recorded for pDCPD upon aging under elevated temperatures.[7] Products made from pDCPD typically display excellent impact strength, stiffness, and high resistance to temperature and chemical corrosion. The combination of good mechanical properties and low density makes it attractive for lightweight materials without compromising toughness and strength. These features are important for improving energy efficiencies, for example in automobile and other vehicle designs.[10,11] A broader list of applications of pDCPD includes aerogels,[12–14] self-healing materials,[15,16] glass/carbon-fiber-reinforced composites,[17–20] ballistic protection,[21–23] wind turbine blades manufacturing,[24] and pipeline coatings for the petrochemical industry.[25]

The impressive reactivity and efficiency of transition metal olefin metathesis catalysts introduce the caveat of being too highly active to stop at the linear pDCPD product. In fact, there are few examples reporting the synthesis of linear pDCPD, which use well defined Mo-, W-, Ti-, and Ru-based catalysts in dilute solutions with low initiator loading or the addition of chain transfer agents.[26–33] Although good control over stereoselectivity and tacticity have been achieved in some cases, limitations, such as the requirement of complex setups under an inert atmosphere, high costs, and difficulties for metal initiator preparation, make these strategies impractical outside of academia. Additionally, the residual metals trapped in the polymer may cause side reactions that alter physical properties of the final products.[7]

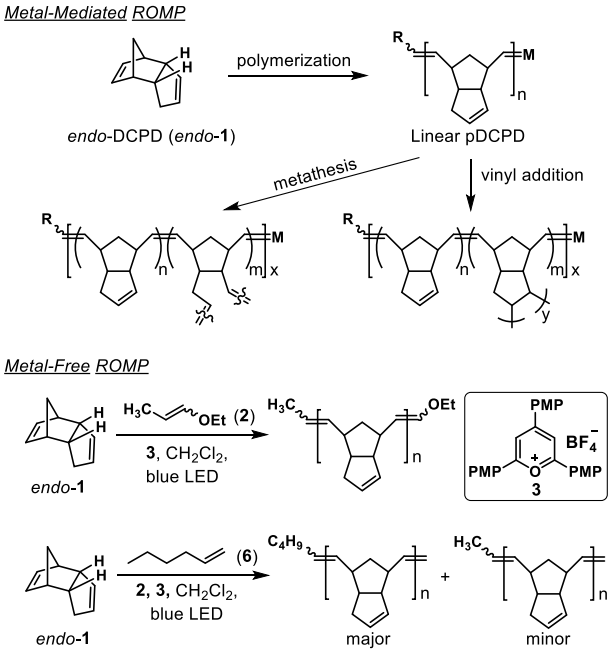

Scheme 1 Summary of Metal-mediated polymerization and cross-linking of *endo*-DCPD vs. metal-free approach for the synthesis of linear *endo*-DCPD polymers and oligomers. PMP = *p*-methoxyphenyl.

[a] *Department of Chemistry, University of Wisconsin-Madison, Madison, WI 53706, USA.*
[b] *Division of Sciences and Mathematics, School of Integrated Arts and Sciences, University of Washington Tacoma, Tacoma, WA 98402, USA.*
[c] *Department of Chemistry, Tulane University, New Orleans, LA 70118, USA.*
[d] *Department of Chemistry, University of Minnesota, Minneapolis, MN 55455, USA.*
[e] *Department of Chemical and Biological Engineering, Department of Materials Science and Engineering, University of Wisconsin-Madison, Madison, WI 53706, USA.*
Electronic Supplementary Information (ESI) available. See DOI: 10.1039/x0xx00000x

Recently, we reported a photoredox mediated metal-free ROMP (MF-ROMP) using ethyl-1-propenyl ether (**2**) as the initiator and a pyrylium salt (**3**) as photo-oxidant (Scheme 1). To our surprise, this method produced only linear pDCPD without any signs of cross-linking. To our disappointment, monomer conversions were poor, molecular weights were uncontrolled, and degrees of polymerization were low.[34,35] This was unfortunate considering that the potentially vast applications of easily processable linear pDCPD have yet to be realized. Motivated by the potential for an efficient synthesis of linear pDCPD, access to controlled molecular weights, fundamental structure-property relationships, and better processability, we revisited the MF-ROMP of DCPD. Generation of radical cationic intermediates on the polycyclic DCPD framework invites numerous side reactions, such as cyclization[36–40] and rearrangement,[41–45] which likely introduce early irreversible termination. From our perspective, the most important and practical goal was to use straightforward reaction engineering to circumvent deleterious pathways. Herein, we report breakthroughs for the efficient synthesis of linear pDCPD, as well as fundamental studies of the MF-ROMP polymerization kinetics of isomeric DCPD monomers, properties of linear pDCPD products, and application of chain transfer agents for controlled synthesis of oligomeric products.

Results and discussion

Unlike the MF-ROMP of norbornene (**4**) that reaches high conversion (>80%) even in large scale synthesis,[46] the MF-ROMP of *endo*-DCPD was initially found to be underperforming. Typically, low molecular weight linear pDCPD (M_n < 6 kDa) was produced with relatively low monomer conversion (13–15%).[34] Attempts at chain extension, successive additions of photo-oxidant, and increased reaction time were each met with limited success. Notably, portion-wise addition of enol ether initiator was found to incrementally increase monomer conversion, consistent with irreversible termination being the major impediment, but this approach is cumbersome on production scale and sacrifices control over pDCPD molecular weight. In our previous attempted optimization, carrying out the polymerization at 4 °C gave a slight improvement in conversion to 20%. We thus focused on varying temperature, initial monomer concentration ($[M]_o$), and initial ratio of monomer to initiator ($[M]_o/[I]_o$) in an attempt to maximize the relative rate of propagation in comparison with termination events. For comparison with standard conditions, MF-ROMP of *endo*-DCPD carried out at 22 °C and an $[M]_o$ = 1.73 M gave 24% conversion and a pDCPD product with M_n = 5.61 kDa (Table 1, entry 1). When carried out in more dilute solution ($[M]_o$ = 0.88 M) at -29 °C, the polymerization reached 47% conversion and yielded linear pDCPD with an M_n = 15.8 kDa (Table 1, entry 2).

To gain insight into how the $[M]_o/[I]_o$, $[M]_o$, and temperature impact MF-ROMP of *endo*-DCPD, we screened these parameters concurrently. At low temperature (-29 °C), the conversion of *endo*-DCPD increased dramatically from 47% to almost 100% as the $[M]_o/[I]_o$ was decreased incrementally from 100:1 to 10:1 (Table 1, entry 2, 6, 11 and 14). Unlike our previous results,[34] decreasing $[M]_o$ significantly improved the conversion at low temperature. This was most prevalent at lower $[M]_o/[I]_o$ (Table 1 and Fig. 1a). The more distinguishable amelioration of conversion is likely due to changes in solvent effect as seen in our previous studies;[47,48] *endo*-DCPD is coincidentally less polar than CH_2Cl_2 solvent, which impairs the radical cationic polymerization process.[49–51] We hypothesize that the radical cationic active chain end exists as part of a radical-ion pair with the pyrylium counteranion and the pyranyl radical. CH_2Cl_2 can better solvate the charge separated radical cationic species than can the *endo*-DCPD monomer. Therefore, decreasing $[M]_o$ creates a solution with higher polarity that can accelerate the formation of solvent-separated radical-ion pair

Table 1 MF-ROMP of *endo*-DCPD optimization at low temperature by varying $[M]_o$.

entry	$[endo\text{-}\mathbf{1}]_o$ (M)	*endo*-**1**:**2**:**3**[a]	temp (°C)	conv (%)[b]	$M_{n,theo}$ (kDa)[c]	$M_{n,exp}$ (kDa)[d]	$M_{w,exp}$ (kDa)[d]	$Đ$[d]	IE (%)[e]
1	1.73	100:1:0.07	22	24	3.29	5.61	7.93	1.4	59
2	0.88	100:1:0.07	-29	47	6.25	15.8	21.6	1.4	40
3	2.59	50:1:0.07	-29	9	0.69	2.57	3.60	1.4	27
4	2.13	50:1:0.07	-29	32	2.23	5.56	9.52	1.7	40
5[f]	1.57	50:1:0.07	-29	61	4.10	12.5	20.1	1.6	33
6	0.88	50:1:0.07	-29	70	4.71	11.4	16.6	1.5	41
7[f]	0.47	50:1:0.07	-29	66	4.42	9.48	12.7	1.3	47
8	2.57	25:1:0.03	-29	25	0.92	2.55	3.91	1.5	36
9	2.12	25:1:0.03	-29	49	1.71	4.08	6.50	1.6	42
10	1.59	25:1:0.07	-29	75	2.55	6.73	10.8	1.6	38
11[f]	0.88	25:1:0.07	-29	91	3.08	8.62	14.4	1.7	36
12	0.48	25:1:0.07	-29	89	3.02	8.02	12.2	1.5	38
13	1.55	10:1:0.03	-29	74	1.06	2.69	4.29	1.6	40
14	0.88	10:1:0.05	-29	100	1.41	5.04	8.28	1.6	28
15	0.47	10:1:0.05	-29	97	1.37	4.10	6.29	1.5	33

[a]Initial molar ratio of *endo*-**1**, **2**, and **3**. [b]Conversion determined by ^{1}H NMR spectroscopy. [c]Theoretical number-average molecular weight (M_n) based upon $[endo\text{-}\mathbf{1}]_o/[\mathbf{2}]_o$ and monomer conversion. [d]Determined by GPC analysis on crude reaction sample using multi-angle light scattering (MALS) and refractive index (RI) detection. Dispersity ($Đ$) = M_w/M_n. [e]Initiation efficiency (IE) = $M_{n,theo}/M_{n,exp}$. [f]Average of thdree runs. All reactions were conducted in CH_2Cl_2 for 60 min.

Table 2 MF-ROMP of *endo*-DCPD optimization by varying temperature and $[M]_o/[I]_o$.

entry	$[endo\text{-}\mathbf{1}]_o$ (M)	*endo*-**1**:**2**:**3**[a]	temp (°C)	conv (%)[b]	$M_{n,theo}$ (kDa)[c]	$M_{n,exp}$ (kDa)[d]	$M_{w,exp}$ (kDa)[d]	$Đ$[d]	IE (%)[e]
1	0.88	100:1:0.07	-29	47	6.25	15.8	21.6	1.4	40
2	0.89	100:1:0.07	-11	58	7.75	18.0	26.3	1.5	43
3	0.88	100:1:0.07	3	36	4.87	8.40	11.3	1.3	58
4	0.88	100:1:0.07	22	24	3.29	5.37	6.99	1.3	61
5	0.88	50:1:0.07	-29	70	4.71	11.4	16.6	1.5	41
6	0.88	50:1:0.07	-11	74	4.94	9.68	14.5	1.5	51
7[f]	0.88	50:1:0.07	3	70	4.68	8.89	13.5	1.5	53
8	0.88	50:1:0.07	22	41	2.80	4.67	6.52	1.4	60
9[f]	0.88	25:1:0.07	-29	91	3.08	8.62	14.4	1.7	36
10	0.88	25:1:0.07	-11	93	3.14	8.51	13.7	1.6	37
11[f]	0.88	25:1:0.07	3	89	3.03	6.49	9.65	1.5	47
12	0.88	25:1:0.07	22	54	1.86	3.15	4.36	1.4	59
13	0.88	10:1:0.05	-29	100	1.41	5.04	8.28	1.6	28
14	0.88	10:1:0.05	-11	100	1.41	3.49	5.40	1.6	40
15	0.88	10:1:0.05	3	94	1.33	2.60	3.49	1.3	51
16	0.87	10:1:0.05	22	63	0.92	1.44	1.96	1.4	64

[a]Initial molar ratio of *endo*-**1**, **2**, and **3**. [b]Conversion determined by ^{1}H NMR spectroscopy. [c]Theoretical M_n based upon $[endo\text{-}\mathbf{1}]_o/[\mathbf{2}]_o$ and monomer conversion. [d]Determined by GPC analysis on crude reaction sample using MALS and RI detection. [e]IE = $M_{n,theo}/M_{n,exp}$. [f]Average of three runs. All reactions were conducted in CH_2Cl_2 for 60 min.

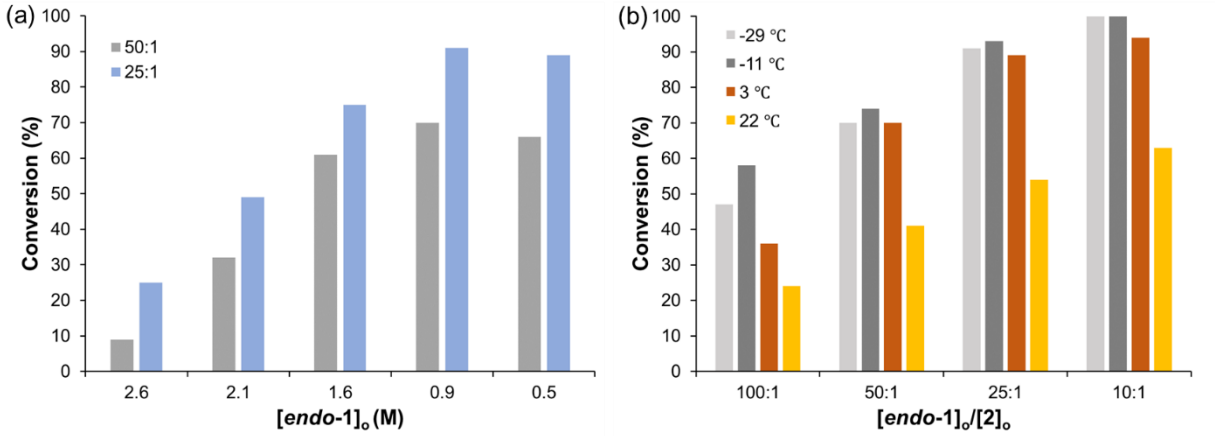

Fig. 1 Summary of (a) $[M]_o$ effect ($[endo\text{-}\mathbf{1}]_o/[\mathbf{2}]_o$ = 50:1 and 25:1, respectively, at -29 °C), (b) $[M]_o/[I]_o$ and temperature effects ($[endo\text{-}\mathbf{1}]_o$ = 0.88 M) on polymerization of *endo*-**1** (see details in Table 1–2).

(SSRIP), in-turn making propagation more favorable.[52] Conversely, in a less polar solution with high $[M]_o$, the formation of contact radical-ion pair (CRIP) is favorable, facilitating the back electron transfer (deactivation of the chain end) and limiting propagation. Therefore, a low $[M]_o$ is beneficial to achieve high conversion.

We next focused on temperature effects for polymerizations in dilute solutions ($[M]_o$ = 0.88 M) and using systematically varied $[M]_o/[I]_o$ values (Table 2 and Fig. 1b). Low temperature favored propagation, as indicated by higher monomer conversion and pDCPD molecular weights, but led to gelation during polymerization when $[M]_o/[I]_o \geq$ 25:1. Bimodal molecular weight distributions with small shoulders showing very high M_n (>200 kDa) were observed by gel permeation chromatography (GPC) (Fig. S2). We hypothesize that gelation of pDCPD at low temperature (-29 °C) results in inhomogeneous compositional gradients (i.e., gel effects). This could result in inconsistent propagation rates or chain-chain coupling, leading to high M_n shoulders.[35] Increasing the temperature from -29 to -11 °C precluded the gelation and resulted in even higher monomer conversion. Increasing the temperature above -11 °C started to reintroduce diminished monomer conversions, but a temperature range of 0 to 3 °C for MF-ROMP of *endo*-DCPD was identified as a satisfactory compromise between monomer conversion and operational simplicity. Notably, >89% conversion was achieved at 3 °C with low $[M]_o/[I]_o$ of 25:1 and 10:1 (Table 2, entry 11 and 15). Therefore, all further work was done at 3 °C due to ease of accessibility compared to lower reaction temperatures. Although the termination of MF-ROMP has not been well understood, we hypothesized that low temperatures could reduce the rate of termination, the rate of chain end deactivation, or both, thus promoting propagation. On the other hand, pDCPD solutions in dichloromethane, especially for those with high M_n, show high viscosity at low temperature, likely impairing mass transport and lowering the rate of propagation. Therefore, -11 to 3 °C is ideal for $[M]_o/[I]_o$

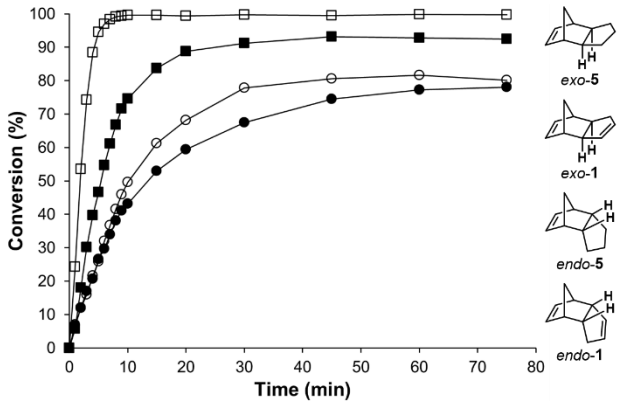

Fig. 2 Plot of conversion vs. time for polymerization of *endo*-**1** (●), *exo*-**1** (■), *endo*-**5** (○) and *exo*-**5** (□) at 3 °C with an $[M]_o/[I]_o$ of 25:1 as determined by ^{1}H NMR spectroscopy.

> 25:1 to reach high monomer conversion as both the termination events and gelation can be minimized. In the cases of very low $[M]_o/[I]_o$ (10:1), gelation was not visibly observed, likely due to the low M_n of the products. As a result, the monomer conversion increased incrementally with a decrease of temperature, from 94% at 3 °C to 100% at -29 °C (Table 2, entries 13–15, Fig. 1b).

In our previous report, MF-ROMP of *endo*-**1**, *exo*-**1**, as well as the *endo*- and *exo*-isomers of dihydroDCPD (*endo*-**5** and *exo*-**5**, respectively) were each investigated to compare their performance under unoptimized conditions ($[M]_o/[I]_o$ = 100:1 and room temperature).[34] The relative MF-ROMP activities was in the order of *exo*-**5** > *endo*-**5** > *exo*-**1** ≈ *endo*-**1** as determined by their initial rates (0.12, 0.037, 0.0063 and 0.0098 min^{-1}, respectively, as shown in Fig. S5 and Table S7). Using the newly optimized conditions $[M]_o/[I]_o$ = 25:1 and 3 °C bath temperature, higher initial rates were observed (k_{obs} = 0.058, 0.15, 0.067 and 0.65 min^{-1} for *endo*-**1**, *exo*-**1**, *endo*-**5** and *exo*-**5**, respectively, as shown in Fig. S4 and Table S6) and higher conversions were achieved, especially for *endo*-**1**, *exo*-**1**, and *endo*-**5** (Fig. 2). Moreover, *exo*-**1** performed significantly better than *endo*-**1**, and the monomer activity under the new conditions was *exo*-**5** > *exo*-**1** > *endo*-**5** > *endo*-**1**, more closely resembling the result of metal-mediated ROMP that is primarily ascribed to steric interactions.[53] The poor solubility of poly(*endo*-**5**) in dichloromethane may have precluded full conversion of the monomer.

Better performance was also seen in the copolymerization of *endo*-**1** and norbornene (**4**), allowing for more efficient preparation of copolymers with high pDCPD content. In our previous work, the overall conversion decreased dramatically with an increased feeding ratio of *endo*-**1**.[34] This was remedied herein by carrying out the polymerization via optimized conditions at 3 °C. When using a 1:1 molar feed ratio of *endo*-**1** and **4**, a total conversion of 91% was achieved, as compared to 29% in our previous report (Table S2). Comparison of initial rates of polymerization for each monomer offers preliminary support for a statistical copolymerization (Fig. S6). The final copolymer was comprised of 46% pDCPD, suggesting a slightly higher rate of incorporation of **4**.

Low M_n oligomers are more processable than their high M_n counterparts, for example in reaction injection molding, and could therefore be good alternatives to volatile small molecule resins. Also, oligomeric thermoset materials have been applied as sizing packages for fiber-reinforced composites. We obtained linear pDCPD in high conversions with M_n values from 1.44 to 18.0 kDa by varying the $[M]_o/[I]_o$ and using the new MF-ROMP conditions. To further tune the M_n, and to avoid cationic homopolymerization of the enol ether initiator (**2**) at high $[M]_o/[I]_o$, we introduced 1-hexene (**6**) as a chain transfer agent (CTA), analogous to our recently reported procedure using **4** as monomer (Scheme 1).[47] Notably, the chain transfer approach would be significantly impeded using our previously reported MF-ROMP of *endo*-DCPD, which suffered early and irreversible termination. The improved reaction conditions provide sustained propagation, thus potentiating successful chain transfer and catalytic use of the enol ether moiety.

By varying the amount of **6** from 0 to 50 equivalents relative to **2**, the M_n values were successfully reduced from 6.49 to 1.00 kDa (determined by GPC analysis on crude reaction samples) (Table S1). It was found that the effective initiation efficiency (IE) dramatically increased with the loading of **6**, consistent with catalytic turnover of the vinyl ether groups. Moreover, the resulting oligomer with a terminal alkene and alkyl group (C_4H_9) instead of a vinyl ether chain end could be clearly assigned by ^{1}H NMR spectroscopy (Fig. S14–S18). These results indicated to us that chain transfer was occurring through cross metathesis with the active chain end. The degree of polymerization (DP), as determined from ^{1}H NMR spectroscopy by comparing the integration of polymer and chain ends, were found to be in close agreement with the results obtained by GPC (Table S4).

The polymer structure was further confirmed by matrix-assisted laser-desorption ionization time-of-flight mass spectrometry (MALDI-TOF MS). For low M_n pDCPD prepared using **6** as CTA, we observed *n*-mers of pDCPD with spacing of

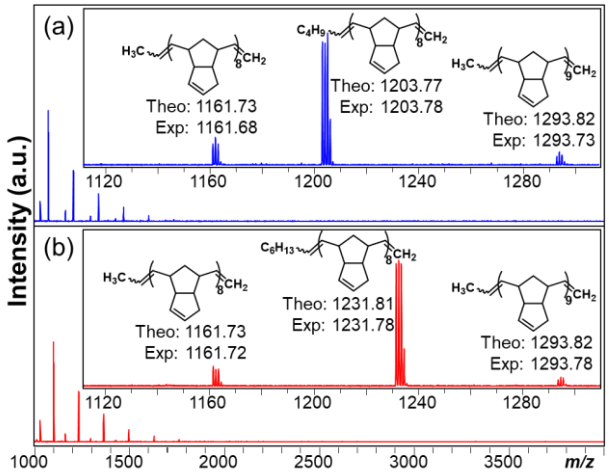

Fig. 3 MALDI-TOF mass spectra with insert spectra from *m/z* = 1110 to 1310 showing *endo*-DCPD oligomers prepared by using (a) **6** and (b) **7** as CTA, respectively. The spectra were taken in positive reflector mode, and all labeled signals represent adducts via $^{63}Cu^+$ ionization.

132.05 *m/z*, consistent with the repeat unit theoretical monoisotopic mass of 132.09 *m/z* (Fig. 3). The peak at 1203.78 *m/z* correlates to an oligomer with a terminal alkene and a C_4H_9 alkyl chain end, consistent with the ^{1}H NMR analysis (Fig. S15–S18). Another product appears at 1161.68 *m/z* and is considered to be one having a terminal alkene and a methyl end group, which should be generated by initiation of **2** followed by cross metathesis of the enol ether chain end with **6**. This regioselectivity of chain transfer is consistent with our previous report.[47] Analogous results were observed by analyzing the oligomers prepared using 1-octene (**7**) as CTA. To further validate our end group assignments, the above oligomers were ionized with different cations, resulting in signals corresponding to the same structures as those shown here (Fig. S7).

As mentioned previously, the overwhelming majority of thermal properties studies on pDCPD have been with cross-linked thermoset materials, which show T_g values > 114 °C.[5–7] In comparison, linear pDCPD has a much lower reported T_g value of ca. 53 °C.[26] T_g is a useful indicator for the thermal and mechanical properties of pDCPD, as well as its operating and service temperature.[25] We envision that using linear pDCPD can improve the manipulability to control over T_g, and the high-performance properties of thermosets can be delivered by a downstream cross-linking. Additionally, linear pDCPD with appropriate molecular weight (M_n) and viscosity can facilitate the processibility of liquid resin in molding and potentially 3D printing for industrial manufacturing. With an efficient means to synthesize linear pDCPD with controlled molecular weights, we seized the opportunity to investigate structure-thermal property relationships.

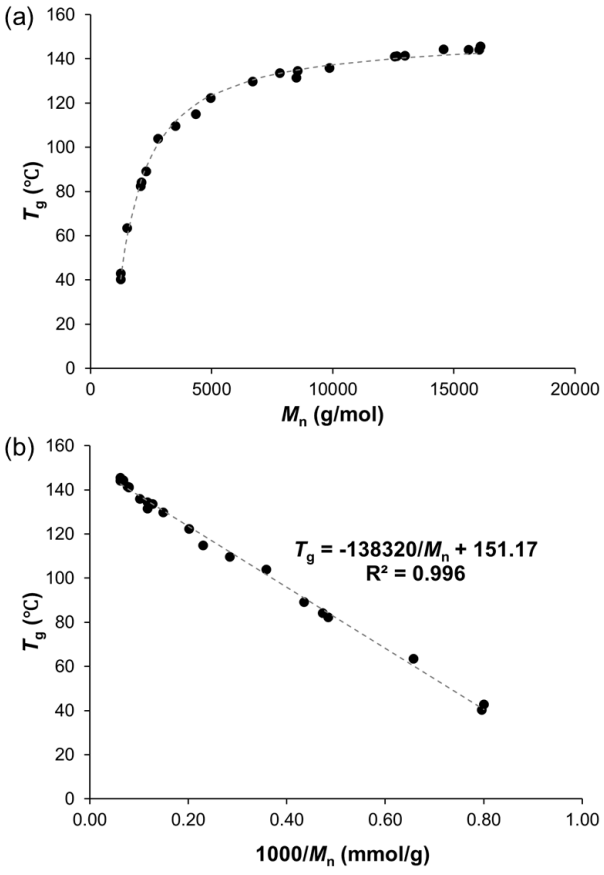

Fig. 4. Dependence of T_g on M_n for polymeric and oligomeric *endo*-DCPD samples. (a) Plot of T_g vs. M_n. (b) Plot of T_g vs. M_n^{-1} using equation 1 to determine $T_{g,\infty}$.

The thermal properties of a series of polymeric and oligomeric *endo*-DCPD with M_n from 1.25 to 16.1 kDa were examined by thermogravimetric analysis (TGA) and differential scanning calorimetry (DSC). The decomposition temperature (T_d) of each sample was determined by the onset of the weight loss from TGA thermograms. The values ranged from 433–438 °C under nitrogen, and 427–437 °C under air, without showing any dependence upon M_n. Notably, minor weight loss around 310–330 °C was observed for *endo*-DCPD oligomers (e.g., about 5% weight loss for a 1.25 kDa oligomer as shown in Fig. S8a). This lower temperature weight loss is probably due to the loss of chain ends, which comprise higher proportions of the total weight for smaller oligomers (Table S8). However, we cannot rule out lower M_n oligomers as the source.

The T_g values of most linear polymers show positive correlation to their DP at sufficiently low M_n regime. These relationships are summarized by the Flory-Fox equation (equation 1) based on the concept that chain ends lead to more free volume than *n*-mer units in the polymer backbone.[54,55] In this equation, $T_{g,\infty}$ is the asymptotic value of T_g at infinite M_n and K is an empirical parameter for a particular polymer species. The K value is small for a highly flexible polymer, while a rigid polymer exhibits large K value, indicating a strong T_g–M_n dependence.

$$T_g = T_{g,\infty} - \frac{K}{M_n} \quad (1)$$

The T_g of linear pDCPD prepared by MF-ROMP ranged from 40 to 145 °C, as measured by DSC under a nitrogen atmosphere (Table S3 and Fig. 4a). Fig. 4b shows a linear correlation between T_g and M_n^{-1}, and a $T_{g,\infty}$ of 151 °C was estimated for linear pDCPD, which appeared in the range of reported T_g values for cross-linked pDCPD.[5–7]

Equation (1) is mostly accurate for polymers with high M_n and narrow molecular weight distribution ($Đ$), but may introduce inaccuracy for certain polymers having low M_n and broad $Đ$. In this scenario, equation (2) can be used for correction.[56] The plot of T_g vs. $(M_nM_w)^{-1/2}$ also showed a good linearity (R^2 = 0.992 as shown in Fig. S10), and the $T_{g,\infty}$ (150 °C) was close to what was determined from equation (1).

$$T_g = T_{g,\infty} - \frac{K}{(M_nM_w)^{1/2}} \quad (2)$$

We noted that the characteristics associated with the chain end such as size, polarity, and flexibility should not be neglected, especially for very short oligomers. A recent study showed that the chain end structure had a significant effect on T_g of linear polystyrene at low M_n regime and the K value obtained from the Flory-Fox equation.[57] The long, flexible chain ends dramatically reduced bulk T_g, while chain ends with bulkiness and hydrogen bonding capabilities resulted in very weak M_n dependence on T_g. In our study, the effect by changing the chain end from vinyl ether to alkyl group (C_4H_9 or C_6H_{13}) might be trivial as we saw a good T_g–M_n correlation, although

further study is required to explain the influence of the chain ends in detail.

We consistently observed an exotherm during the first heating cycle of DSC, right before the occurrence of the glass transition. We speculated that this peak is related to polymer annealing or thermal cross-linking.[3–5,58–60] Although the DSC measurement is performed under nitrogen, trace amounts of oxygen may be trapped inside the sample during preparation, thus enabling thermal-oxidative aging of pDCPD. Side reactions related to thermal-oxidative processes, including post-curing, carbonyl growth and chain scission, can each influence the bulk T_g.[61] Studies on pDCPD oxidation have shown that when a specimen was aged under air at high temperatures, an oxidized thin layer was found to form on the surface, limiting progressive oxidation into the bulk.[25] Therefore, the inner bulk material remained unaffected. Considering the potential trace amount of oxygen in our case, along with the diffusion-limited oxidation mechanism and a fast consumption rate of oxygen,[62] the influence from thermal oxidation should be insignificant.

After successive heating and cooling DSC cycles, the bulk T_g increased by approximately 1 ℃ in most cases. To discern if thermal cross-linking happened during heating cycles, the sample was cured at 150 ℃ under nitrogen atmosphere for 1 hour followed by GPC characterization. For comparison, the same sample cured under DSC measurement was also characterized (see Table S9–S10 and Fig. S9 in detail). In each case, the cured *endo*-DCPD oligomer with M_n = 1.25 kDa was soluble in THF and no significant change of M_n (from 1.25 to 1.25 and 1.25 to 1.10 kDa, respectively) was observed. Notably, a polymer sample with M_n = 14.6 kDa only partially dissolved in THF or CH_2Cl_2 after both curing processes. Bimodality, broadened $Đ$, and increased M_n (from 14.6 to 14.8 and 14.6 to 34.9 kDa, respectively) were observed from GPC analysis. These results indicated to us that thermally induced cross-linking likely occurred within a small portion of the sample during curing processes.[3–5,58] The physical properties of the *endo*-DCPD polymer and oligomer at elevated temperatures (i.e., solid or liquid), as well as the difference of oxygen levels under the two curing processes may account for the observations as shown above. Overall, the T_g measured by DSC under nitrogen could represent the bulk T_g of linear pDCPD, despite the slow aging process that occurs.

Conclusions

In conclusion, we have developed a revised and highly efficient synthesis of linear pDCPD using photoredox mediated MF-ROMP. High conversions (>89%) and controlled molecular weights, including oligomeric materials, are now accessible in a straightforward manner. The high fidelity of the chain ends allowed for introduction of chain transfer agents to modulate the M_n and control the end group structure. With the ability to control the polymerization of *endo*-DCPD, we were able to evaluate T_g–M_n dependence of linear pDCPD for the first time. Since the effect of each reaction parameter (temperature, $[M]_o$, and $[M]_o/[I]_o$) on the relative rates of propagation and termination has not been completely elucidated, further studies to probe the reaction mechanism are required. In addition, thermal and mechanical properties of linear pDCPD as well as aging studies are underway.

Conflicts of interest

A.J.B. has an ownership interest in Boydston Chemical Innovations, Incorporated, which has licensed the technology reported in this publication.

Acknowledgements

We gratefully acknowledge financial support from the Army Research Labs (Cooperative Agreement No. W911NF-17-2-0199), the National Science Foundation (DMR-1452726 and CHE-2002886), and Boydston Chemical Innovations, Inc. A.J.B. acknowledges partial financial support from the Yamamoto Family, the Office of the Vice Chancellor for Research and Graduate Education at the University of Wisconsin – Madison with funding from the Wisconsin Alumni Research Foundation. The following instrumentation in the Paul Bender Chemical Instrumentation Center was sup-ported by: Bruker AVANCE 400 NMR spectrometer by NSF CHE-1048642; Bruker AVANCE 500 NMR spectrometer by a generous gift from Paul J. and Margaret M. Bender. The Grayson group acknowledges support for the MALDI-TOF MS from the National Science Foundation MRI CHE-0619770.

Notes and references

1 V. Dragutan, I. Dragutan and M. Dimonie, in *Green Metathesis Chemistry, NATO Science for Peace and Security Series A: Chemistry and Biology*, Springer, Dordrecht, 2010, pp. 369–381.
2 R. A. Fisher and R. H. Grubbs, *Makromol. Chemie. Macromol. Symp.*, 1992, **63**, 271–277.
3 T. A. Davidson, K. B. Wagener and D. B. Priddy, *Macromolecules*, 1996, **29**, 786–788.
4 T. A. Davidson and K. B. Wagener, *J. Mol. Catal. A Chem.*, 1998, **133**, 67–74.
5 T. J. Cuthbert, T. Li, A. W. H. Speed and J. E. Wulff, *Macromolecules*, 2018, **51**, 2038–2047.
6 T. K. H. Trinh, G. Schrodj, S. Rigolet, J. Pinaud, P. Lacroix-Desmazes, L. Pichavant, V. Héroguez and A. Chemtob, *RSC Adv.*, 2019, **9**, 27789–27799.
7 Y. Vidavsky, Y. Navon, Y. Ginzburg, M. Gottlieb and N. Gabriel Lemcoff, *Beilstein J. Org. Chem.*, 2015, **11**, 1469–1474.
8 X. Sheng, J. K. Lee and M. R. Kessler, *Polymer*, 2009, **50**, 1264–1269.
9 R. S. Phatake, A. Masarwa, N. G. Lemcoff and O. Reany, *Polym. Chem.*, 2020, **11**, 1742–1751.
10 D. Vervacke, *An Introduction to PDCPD: Poly-Di-Cyclo-Penta-Diene*, Product Rescue, Waarschoot, Belgium, 2008.
11 S. Kovačič and C. Slugovc, *Mater. Chem. Front.*, 2020, **4**, 2235–2255.
12 J. K. Lee and G. L. Gould, *J. Sol-Gel Sci. Technol.*, 2007, **44**, 29–40.
13 J. M. Lenhardt, S. H. Kim, M. A. Worsley, R. N. Leif, P. G. Campbell, T. F. Baumann and J. H. Satcher, *J. Non-Cryst. Solids*, 2015, **408**, 98–101.

14 J. M. Lenhardt, S. H. Kim, A. J. Nelson, P. Singhal, T. F. Baumann and J. H. Satcher, *Polymer*, 2013, **54**, 542–547.
15 S. R. White, N. R. Sottos, P. H. Geubelle, J. S. Moore, M. R. Kessler, S. R. Sriram, E. N. Brown and S. Viswanathan, *Nature*, 2001, **409**, 794–797.
16 J. D. Rule, E. N. Brown, N. R. Sottos, S. R. White and J. S. Moore, *Adv. Mater.*, 2005, **17**, 205–208.
17 S. E. Boyd, *Mechanical and Impact Characterization of Poly-Dicyclopentadiene (p-DCPD) Matrix Composites Using Novel Glass Fibers and Sizings*, ARL-TR-7749, US Army Research Laboratory, 2016.
18 S. Vyas, E. Goli, X. Zhang and P. H. Geubelle, *Compos. Sci. Technol.*, 2019, **184**, 107832.
19 I. D. Robertson, M. Yourdkhani, P. J. Centellas, J. E. Aw, D. G. Ivanoff, E. Goli, E. M. Lloyd, L. M. Dean, N. R. Sottos, P. H. Geubelle, J. S. Moore and S. R. White, *Nature*, 2018, **557**, 223–227.
20 H. M. Yoo, M. S. Kim, B. S. Kim, D. J. Kwon and S. W. Choi, *e-Polymers*, 2019, **19**, 437–443.
21 D. B. K. Jr, K. A. Masser, R. M. Elder, T. W. Sirk, M. D. Hindenlang, J. H. Yu, A. D. Richardson, S. E. Boyd, W. A. Spurgeon and J. L. Lenhart, *Compos. Sci. Technol.*, 2015, **114**, 17–25.
22 T. R. Long, R. M. Elder, E. D. Bain, K. A. Masser, T. W. Sirk, J. H. Yu, D. B. Knorr and J. L. Lenhart, *Soft Matter*, 2018, **14**, 3344–3360.
23 R. M. Elder, D. B. Knorr, J. W. Andzelm, J. L. Lenhart and T. W. Sirk, *Soft Matter*, 2016, **12**, 4418–4434.
24 J. F. Mandell, D. D. Samborsky and D. A. Miller, in *Advances in Wind Turbine Blade Design and Materials*, eds. P. Brøndsted and R. P. L. Nijssen, Woodhead Publishing, 2013, pp. 210–250.
25 P. Y. Le Gac, D. Choqueuse, M. Paris, G. Recher, C. Zimmer and D. Melot, *Polym. Degrad. Stab.*, 2013, **98**, 809–817.
26 M. J. Abadie, M. Dimonie, C. Couve and V. Dragutan, *Eur. Polym. J.*, 2000, **36**, 1213–1219.
27 B. Autenrieth, H. Jeong, W. P. Forrest, J. C. Axtell, A. Ota, T. Lehr, M. R. Buchmeiser and R. R. Schrock, *Macromolecules*, 2015, **48**, 2480–2492.
28 S. Hayano, H. Kurakata, Y. Tsunogae, Y. Nakayama, Y. Sato and H. Yasuda, *Macromolecules*, 2003, **36**, 7422–7431.
29 S. Hayano, Y. Takeyama, Y. Tsunogae and I. Igarashi, *Macromolecules*, 2006, **39**, 4663–4670.
30 K. Dono, J. Huang, H. Ma and Y. Qian, *J. Appl. Polym. Sci.*, 2000, **77**, 3247–3251.
31 N. D. Steese, D. Barvaliya, X. D. Poole, D. E. McLemore, J. C. DiCesare and H. J. Schanz, *J. Polym. Sci. Part A: Polym. Chem.*, 2018, **56**, 359–364.
32 C. Dumrath, A. Dumrath, H. Neumann, M. Beller and R. Kadyrov, *ChemCatChem*, 2014, **6**, 3101–3104.
33 Z. Yao, Z. Wang, Y. Yu, C. Zeng and K. Cao, *Polymer*, 2017, **119**, 98–106.
34 A. E. Goetz and A. J. Boydston, *J. Am. Chem. Soc.*, 2015, **137**, 7572–7575.
35 L. M. M. Pascual, A. E. Goetz, A. M. Roehrich and A. J. Boydston, *Macromol. Rapid Commun.*, 2017, **38**, 1600766.
36 T. Miyashi, A. Konno and Y. Takahashi, *J. Am. Chem. Soc.*, 1988, **110**, 3676–3677.
37 J. D. Parrish, M. A. Ischay, Z. Lu, S. Guo, N. R. Peters and T. P. Yoon, *Org. Lett.*, 2012, **14**, 1640–1643.
38 N. J. Gesmundo and D. A. Nicewicz, *Beilstein J. Org. Chem.*, 2014, **10**, 1272–1281.
39 R. Shimizu, Y. Okada and K. Chiba, *Beilstein J. Org. Chem.*, 2018, **14**, 704–708.
40 R. Feng, J. A. Smith and K. D. Moeller, *Acc. Chem. Res.*, 2017, **50**, 2346–2352.
41 T. Shida, T. Momose and N. Ono, *J. Phys. Chem.*, 1985, **89**, 815–820.
42 G. O. Schenck and R. Steinmetz, *Chem. Ber.*, 1963, **96**, 520–525.
43 J. A. Berson, C. J. Olsen and J. S. Walia, *J. Am. Chem. Soc.*, 1960, 82, 5000–5001.
44 S. Jana, C. Guin and S. C. Roy, *J. Org. Chem.*, 2005, **70**, 8252–8254.
45 B. C. Hong, H. I. Sun, Y. J. Shr and K. J. Lin, *J. Chem. Soc. Perkin Trans. 1*, 2000, **2**, 2939–2942.
46 V. K. Kensy, PhD Thesis, University of Washington, 2019.
47 V. K. Kensy, R. L. Tritt, F. M. Haque, L. M. Murphy, D. B. Knorr, S. M. Grayson and A. J. Boydston, *Angew. Chem. Int. Ed.*, 2020, **59**, 9074–9079.
48 X. Yang, S. R. Gitter, A. G. Roessler, P. M. Zimmerman and A. J. Boydston, *Angew. Chem. Int. Ed.*, 2021, DOI: 10.1002/anie.202016393.
49 T. Krappitz, K. Jovic, F. Feist, H. Frisch, V. P. Rigoglioso, J. P. Blinco, A. J. Boydston and C. Barner-Kowollik, *J. Am. Chem. Soc.*, 2019, **141**, 16605–16609.
50 W. P. Todd, J. P. Dinnocenzo, J. L. Goodman, S. Farid, I. R. Gould, S. Farid and I. R. Gould, *J. Am. Chem. Soc.*, 1991, **113**, 3601–3602.
51 M. Martiny, E. Steckhan and T. Esch, *Chem. Ber.*, 1993, **126**, 1671–1682.
52 I. R. Gould and S. Farid, *Acc. Chem. Res.*, 1996, **29**, 522–528.
53 J. D. Rule and J. S. Moore, *Macromolecules*, 2002, **35**, 7878–7882.
54 T. G. Fox and P. J. Flory, *J. Appl. Phys.*, 1950, **21**, 581–591.
55 T. G. Fox and P. J. Flory, *J. Polym. Sci.*, 1954, **14**, 315–319.
56 T. Ogawa, *J. Appl. Polym. Sci.*, 1992, **44**, 1869–1871.
57 L. Zhang, J. A. Marsiglio, T. Lan and J. M. Torkelson, *Macromolecules*, 2016, **49**, 2387–2398.
58 J. Chen, F. P. Burns, M. G. Moffitt and J. E. Wulff, *ACS Omega*, 2016, **1**, 532–540.
59 D. Dimonie, M. Dimonie, V. Munteanu, H. Iovu, J. Couve and M. J. Abadie, *Polym. Degrad. Stab.*, 2000, **70**, 319–324.
60 E. Richaud, P. Y. Le Gac and J. Verdu, *Polym. Degrad. Stab.*, 2014, **102**, 95–104.
61 M. C. Celina, *Polym. Degrad. Stab.*, 2013, **98**, 2419–2429.
62 J. Huang, A. David, P. Y. Le Gac, C. Lorthioir, C. Coelho and E. Richaud, *Polym. Degrad. Stab.*, 2019, **166**, 258–271.